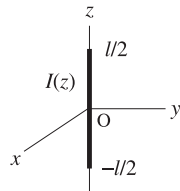# 17

Linear and Loop Antennas

17.1 Linear Antennas

The radiation angular pattern of antennas is completely determined by the transverse component $F_\perp = \hat{\boldsymbol{\theta}} F_\theta + \hat{\boldsymbol{\phi}} F_\phi$ of the radiation vector F, which in turn is determined by the current density J. Here, we consider some examples of current densities describing various antenna types, such as linear antennas, loop antennas, and linear arrays.

For *linear antennas*, we may choose the z-axis to be along the direction of the antenna. Assuming an infinitely thin antenna, the current density will have the form:

$$J(r) = \hat{z} I(z) \delta(x) \delta(y) \qquad \text{(thin linear antenna)} \qquad (17.1.1)$$

where $I(z)$ is the current distribution along the antenna element. It is shown in Sec. 24.4 that $I(z)$ satisfies approximately the Helmholtz equation along the antenna:

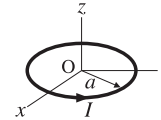$$\frac{d^2 I(z)}{dz^2} + k^2 I(z) = 0 \qquad (17.1.2)$$

Some examples of current distributions $I(z)$ are as follows:

$I(z) = Il\delta(z)$	Hertzian dipole
$I(z) = I$	Uniform line element
$I(z) = I(1 - 2|z|/l)$	Small linear dipole
$I(z) = I \sin(k(l/2 - |z|))$	Standing-wave antenna
$I(z) = I \cos(kz)$	Half-wave antenna ($l = \lambda/2$)
$I(z) = I e^{-jkz}$	Traveling-wave antenna

where l is the length of the antenna element and the expressions are assumed to be valid for $-l/2 \leq z \leq l/2$, so that the antenna element straddles the xy-plane.

The Hertzian dipole, uniform line element, and small linear dipole examples do not satisfy Eq. (17.1.2), except when the antenna length is electrically *short*, that is, $l \ll \lambda$.

For *loop antennas*, we may take the loop to lie on the xy-plane and be centered at the origin. Again, we may assume a thin wire. For a circular loop of radius a, the current flows azimuthally. The corresponding current density can be expressed in cylindrical coordinates $r = (\rho, \phi, z)$ as:

$$J(r) = \hat{\boldsymbol{\phi}} I\delta(\rho - a)\delta(z) \qquad \text{(circular loop)} \qquad (17.1.3)$$

The delta functions confine the current on the $\rho = a$ circle on the xy-plane. We will discuss loop antennas in Sec. 17.8.

Antenna arrays may be formed by considering a group of antenna elements, such as Hertzian or half-wave dipoles, arranged in particular geometrical configurations, such as along a particular direction. Some examples of antenna arrays that are made up from identical antenna elements are as follows:

$$J(r) = \hat{z} \sum_n a_n I(z) \delta(x - x_n)\delta(y) \qquad \text{array along } x\text{-direction}$$

$$J(r) = \hat{z} \sum_n a_n I(z) \delta(y - y_n)\delta(x) \qquad \text{array along } y\text{-direction}$$

$$J(r) = \hat{z} \sum_n a_n I(z - z_n)\delta(x)\delta(y) \qquad \text{array along } z\text{-direction}$$

$$J(r) = \hat{z} \sum_{mn} a_{mn} I(z) \delta(x - x_m)\delta(y - y_n) \qquad \text{2D planar array}$$

The weights a_n, a_{mn} are chosen appropriately to achieve desired directivity properties for the array. We discuss arrays in Sec. 22.1.

It is evident now from Eq. (17.1.1) that the radiation vector F will have only a z-component. Indeed, we have from the definition Eq. (15.7.5):

$$F = \int_V J(r') e^{j\,k\cdot r'}\, d^3 r' = \hat{z} \int I(z')\delta(x')\delta(y') e^{j(k_x x' + k_y y' + k_z z')} dx' dy' dz'$$

The x' and y' integrations are done trivially, whereas the z' integration extends over the length l of the antenna. Thus,

$$F = \hat{z} F_z = \hat{z} \int_{-l/2}^{l/2} I(z') e^{jk_z z'} dz'$$

Using Eq. (15.8.3), the wave vector k can be resolved in cartesian components as:

$$k = k\,\hat{r} = \hat{x} k \cos\phi \sin\theta + \hat{y} k \sin\phi \sin\theta + \hat{z} k \cos\theta = \hat{x} k_x + \hat{y} k_y + \hat{z} k_z$$

Thus,

$$\boxed{\begin{aligned} k_x &= k \cos\phi \sin\theta \\ k_y &= k \sin\phi \sin\theta \\ k_z &= k \cos\theta \end{aligned}} \qquad (17.1.4)$$

It follows that the radiation vector F_z will only depend on the polar angle θ:

$$F_z(\theta) = \int_{-l/2}^{l/2} I(z') e^{jk_z z'} dz' = \int_{-l/2}^{l/2} I(z') e^{jkz' \cos\theta} dz' \qquad (17.1.5)$$

Using Eq. (15.8.2) we may resolve $\hat{\mathbf{z}}$ into its spherical coordinates and identify the radial and transverse components of the radiation vector:

$$\mathbf{F} = \hat{\mathbf{z}} F_z = (\hat{\mathbf{r}} \cos\theta - \hat{\boldsymbol{\theta}} \sin\theta) F_z(\theta) = \hat{\mathbf{r}} F_z(\theta) \cos\theta - \hat{\boldsymbol{\theta}} F_z(\theta) \sin\theta$$

Thus, the transverse component of $\mathbf{F}$ will be have only a θ-component:

$$\mathbf{F}_\perp(\theta) = \hat{\boldsymbol{\theta}} F_\theta(\theta) = -\hat{\boldsymbol{\theta}} F_z(\theta) \sin\theta$$

It follows that the electric and magnetic radiation fields (15.10.5) generated by a linear antenna will have the form:

$$\mathbf{E} = \hat{\boldsymbol{\theta}} E_\theta = \hat{\boldsymbol{\theta}} jk\eta \frac{e^{-jkr}}{4\pi r} F_z(\theta) \sin\theta$$

$$\mathbf{H} = \hat{\boldsymbol{\phi}} H_\phi = \hat{\boldsymbol{\phi}} jk \frac{e^{-jkr}}{4\pi r} F_z(\theta) \sin\theta$$

$$(17.1.6)$$

The fields are *omnidirectional*, that is, independent of the azimuthal angle ϕ. The factor $\sin\theta$ arises from the cartesian to spherical coordinate transformation, whereas the factor $F_z(\theta)$ incorporates the dependence on the assumed current distribution $I(z)$. The radiation intensity $U(\theta, \phi)$ has θ-dependence only and is given by Eq. (16.1.4):

$$U(\theta) = \frac{\eta k^2}{32\pi^2} |F_z(\theta)|^2 \sin^2\theta \qquad \text{(radiation intensity of linear antenna)} \qquad (17.1.7)$$

To summarize, the radiated fields, the total radiated power, and the angular distribution of radiation from a linear antenna are completely determined by the quantity $F_z(\theta)$ defined in Eq. (17.1.5).

17.2 Hertzian Dipole

The simplest linear antenna example is the Hertzian dipole that has a current distribution $I(z) = Il\delta(z)$ corresponding to an infinitesimally small antenna located at the origin. Eq. (17.1.5) yields:

$$F_z(\theta) = \int_{-l/2}^{l/2} I(z') e^{jk_z z'} dz' = \int_{-l/2}^{l/2} Il\delta(z') e^{jkz' \cos\theta} dz' = Il$$

Thus, F_z is a constant independent of θ. The radiation intensity is obtained from Eq. (17.1.7):

$$U(\theta) = \frac{\eta k^2}{32\pi^2} |Il|^2 \sin^2\theta$$

Its maximum occurs at $\theta = \pi/2$, that is, broadside to the antenna:

$$U_{\max} = \frac{\eta k^2}{32\pi^2} |Il|^2$$

It follows that the normalized power gain will be:

$$g(\theta) = \frac{U(\theta)}{U_{\max}} = \sin^2\theta \qquad \text{(Hertzian dipole gain)} \qquad (17.2.1)$$

The gain $g(\theta)$ is plotted in absolute and dB units in Fig. 17.2.1. Note that the 3-dB or half-power circle intersects the gain curve at 45° angles. Therefore, the *half-power beam width* (HPBW) will be 90°—not a very narrow beam. We note also that there is no radiated power *along* the direction of the antenna element, that is, the z-direction, or $\theta = 0$.
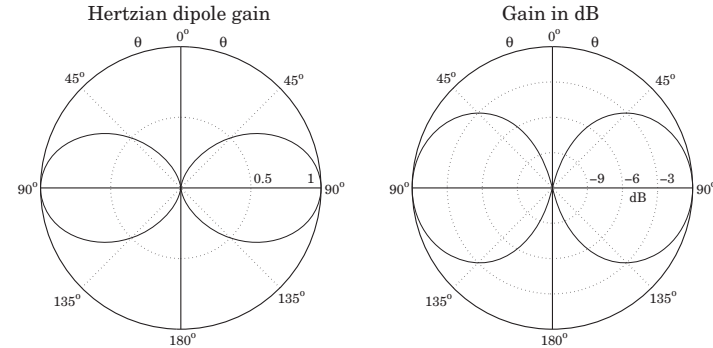

Fig. 17.2.1 Gain of Hertzian dipole in absolute and dB units.

In these plots, the gain was computed by the function `dipole` and plotted with `abp` and `dbp`. For example the left figure was generated by:

```
[g, th, c] = dipole(0, 200);
abp(th, g, 45);
```

Next, we calculate the beam solid angle from:

$$\Delta\Omega = \int_0^\pi \int_0^{2\pi} g(\theta) \sin\theta\, d\theta\, d\phi = 2\pi \int_0^\pi g(\theta) \sin\theta\, d\theta = 2\pi \int_0^\pi \sin^3\theta\, d\theta, \qquad \text{or,}$$

$$\Delta\Omega = \frac{8\pi}{3}$$

It follows that the directivity will be:

$$D_{\max} = \frac{4\pi}{\Delta\Omega} = \frac{4\pi}{8\pi/3} = 1.5 \equiv 1.76 \text{ dB}$$

The total radiated power is then found from Eq. (16.2.17):

$$P_{\text{rad}} = U_{\max}\Delta\Omega = \frac{\eta k^2}{32\pi^2}|Il|^2\frac{8\pi}{3} = \frac{\eta k^2|Il|^2}{12\pi} \tag{17.2.2}$$

Because of the proportionality to $|I|^2$, we are led to define the *radiation resistance* of the antenna, R_{rad}, as the resistance that would dissipate the same amount of power as the power radiated, that is, we define it through:

$$\boxed{P_{\text{rad}} = \frac{1}{2}R_{\text{rad}}|I|^2} \tag{17.2.3}$$

Comparing the two expressions for P_{rad}, we find:

$$R_{\text{rad}} = \frac{\eta k^2 l^2}{6\pi} = \frac{2\pi\eta}{3}\left(\frac{l}{\lambda}\right)^2 \tag{17.2.4}$$

where we replaced $k = 2\pi/\lambda$. Because we assumed an infinitesimally small antenna, $l \ll \lambda$, the radiation resistance will be very small.

A related antenna example is the finite Hertzian, or uniform line element, which has a constant current I flowing along its entire length l, that is, $I(z) = I$, for $-l/2 \le z \le l/2$. We can write $I(z)$ more formally with the help of the unit-step function $u(z)$ as follows:
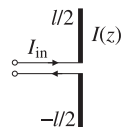
$$I(z) = I\left[u(z + l/2) - u(z - l/2)\right]$$

The Hertzian dipole may be thought of as the limiting case of this example in the limit $l \to 0$. Indeed, multiplying and dividing by l, and using the property that the derivative of the unit-step is $u'(z) = \delta(z)$, we have

$$I(z) = Il\,\frac{u(z + l/2) - u(z - l/2)}{l} \to Il\frac{du(z)}{dz} = Il\delta(z)$$

and we must assume, of course, that the product Il remains finite in that limit.

17.3 Standing-Wave Antennas

A very practical antenna is the center-fed standing-wave antenna, and in particular, the half-wave dipole whose length is $l = \lambda/2$. The current distribution along the antenna length is assumed to be a standing wave, much like the case of an open-ended parallel wire transmission line. Indeed, as suggested by the figure below, the center-fed dipole may be thought of as an open-ended transmission line whose ends have been bent up and down. The current distribution is:

$$I(z) = I\sin\left(k(l/2 - |z|)\right) \qquad \text{(standing-wave antenna)} \tag{17.3.1}$$

Defining the half-length $h = l/2$, the radiation vector z-component $F_z(\theta)$ is:

$$F_z(\theta) = \int_{-h}^{h} I\sin\left(k(l/2 - |z'|)\right)e^{jkz'\cos\theta}dz' = \frac{2I}{k}\frac{\cos(kh\cos\theta) - \cos(kh)}{\sin^2\theta}$$

Inserting $F_z(\theta)$ into Eq. (17.1.7), and canceling some common factors, we obtain:

$$U(\theta) = \frac{\eta|I|^2}{8\pi^2}\left|\frac{\cos(kh\cos\theta) - \cos(kh)}{\sin\theta}\right|^2 \tag{17.3.2}$$

It follows that the normalized power gain $g(\theta)$ will have a similar form:

$$g(\theta) = c_n\left|\frac{\cos(kh\cos\theta) - \cos(kh)}{\sin\theta}\right|^2 \qquad \text{(normalized gain)} \tag{17.3.3}$$

where c_n is a normalization constant chosen to make the maximum of $g(\theta)$ equal to unity. Depending on the value of l, this maximum may not occur at $\theta = \pi/2$.

In the limit $l \to 0$, we obtain the gain of the Hertzian dipole, $g(\theta) = \sin^2\theta$. For small values of l, we obtain the linear-current case. Indeed, using the approximation $\sin x \simeq x$, the current (17.3.1) becomes:

$$I(z) = Ik\left(\frac{l}{2} - |z|\right), \qquad -\frac{l}{2} \le z \le \frac{l}{2}$$

For a general dipole of length l, the current at the input terminals of the antenna is not necessarily equal to the peak amplitude I. Indeed, setting $z = 0$ in (17.3.1) we have:

$$I_{\text{in}} = I(0) = I\sin(kl/2) = I\sin kh \tag{17.3.4}$$

The radiation resistance may be defined either in terms of the peak current or in terms of the input current through the definitions:

$$P_{\text{rad}} = \frac{1}{2}R_{\text{peak}}|I|^2 = \frac{1}{2}R_{\text{in}}|I_{\text{in}}|^2 \quad \Rightarrow \quad R_{\text{in}} = \frac{R_{\text{peak}}}{\sin^2 kh} \tag{17.3.5}$$

When l is a half-multiple of λ, the input and peak currents are equal and the two definitions of the radiation resistance are the same. But when l is a multiple of λ, Eq. (17.3.4) gives zero for the input current, which would imply an infinite input resistance R_{in}. In practice, the current distribution is only approximately sinusoidal and the input current is not exactly zero.

The input impedance of an antenna has in general both a resistive part R_{in} and a reactive part X_{in}, so that $Z_{\text{in}} = R_{\text{in}} + jX_{\text{in}}$. The relevant theory is discussed in Sec. 25.3. Assuming a sinusoidal current, Z_{in} can be computed by Eq. (25.3.10), implemented by the MATLAB function `imped`:

```
Zin = imped(l,a);        % input impedance of standing-wave antenna
```

where l, a are the length and radius of the antenna in units of λ. For example, a half-wave dipole ($l = \lambda/2$) with zero radius has $Z_{\text{in}} = \text{imped}(0.5, 0) = 73.1 + j\,42.5\ \Omega$.

For $l \gg a$, the input resistance remains largely independent of the radius a. The reactance has a stronger dependence on a. Fig. 17.3.1 shows a plot of R_{in} and X_{in} versus
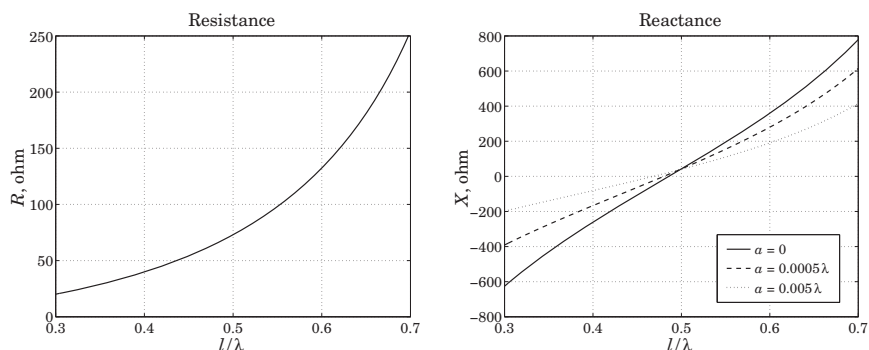
Fig. 17.3.1 Input impedance of standing-wave dipole antenna.

the antenna length l plotted over the interval $0.3\lambda \le l \le 0.7\lambda$, for the three choices of the radius: $a = 0$, $a = 0.0005\lambda$, and $a = 0.005\lambda$.

We observe that the reactance X_{in} vanishes for lengths that are a little shorter than $l = \lambda/2$. Such antennas are called *resonant antennas* in analogy with a resonant RLC circuit whose input impedance $Z = R + j(\omega L - 1/\omega C)$ has a vanishing reactance at its resonant frequency $\omega = 1/\sqrt{LC}$.

For the three choices of the radius a, we find the following resonant lengths and corresponding input resistances:

$$
\begin{aligned}
a &= 0, & l &= 0.4857\lambda, & R_{\text{in}} &= 67.2\ \Omega \\
a &= 0.0005\lambda, & l &= 0.4801\lambda, & R_{\text{in}} &= 65.0\ \Omega \\
a &= 0.005\lambda, & l &= 0.4681\lambda, & R_{\text{in}} &= 60.5\ \Omega
\end{aligned}
$$

An analytical expression for the peak and input radiation resistances can be obtained by integrating the radiation intensity (17.3.2) over all solid angles to get the total radiated power:

$$
P_{\text{rad}} = \int U(\theta)\, d\Omega = \int_0^\pi \int_0^{2\pi} U(\theta) \sin\theta\, d\theta\, d\phi = 2\pi \int_0^\pi U(\theta) \sin\theta\, d\theta
$$

$$
= \frac{\eta |I|^2}{4\pi} \int_0^\pi \frac{(\cos(kh\cos\theta) - \cos(kh))^2}{\sin\theta}\, d\theta
$$

Comparing with (17.3.5), we obtain the peak resistance:

$$
R_{\text{peak}} = \frac{\eta}{2\pi} \int_0^\pi \frac{(\cos(kh\cos\theta) - \cos(kh))^2}{\sin\theta}\, d\theta
$$

Using the trigonometric identity,

$$
(\cos(kh\cos\theta) - \cos(kh))^2
$$

$$
= \frac{1}{2}(\cos(2kh\cos\theta) - \cos(2kh)) - 2(\cos(kh\cos\theta) - \cos(kh))\cos kh
$$

the above integral can be expressed as a sum of two integrals of the form:

$$
\int_0^\pi \frac{\cos(\alpha\cos\theta) - \cos\alpha}{\sin\theta}\, d\theta = S_i(2\alpha)\sin\alpha - C_{\text{in}}(2\alpha)\cos\alpha
$$

which is derived in Appendix F. This leads to the integral:

$$
\int_0^\pi \frac{(\cos(kh\cos\theta) - \cos(kh))^2}{\sin\theta}\, d\theta =
$$

$$
C_{\text{in}}(kl) + \frac{1}{2}\cos kl\, [2C_{\text{in}}(kl) - C_{\text{in}}(2kl)] + \frac{1}{2}\sin kl\, [S_i(2kl) - 2S_i(kl)]
$$

(17.3.6)

and to the radiation resistance:

$$
R_{\text{peak}} = \frac{\eta}{2\pi}\left[C_{\text{in}}(kl) + \frac{1}{2}\cos kl\, [2C_{\text{in}}(kl) - C_{\text{in}}(2kl)] + \frac{1}{2}\sin kl\, [S_i(2kl) - 2S_i(kl)] \right]
$$

(17.3.7)

which agrees with Eq. (25.3.21) derived by a different method. The radiation resistance R_{peak} also determines the directivity of the dipole antenna. Using (17.3.3) for the normalized gain, we find the beam solid angle:

$$
\Delta\Omega = \int_0^\pi \int_0^{2\pi} g(\theta)\, d\Omega = 2\pi c_n \int_0^\pi \frac{(\cos(kh\cos\theta) - \cos(kh))^2}{\sin\theta}\, d\theta = 2\pi c_n \frac{2\pi R_{\text{peak}}}{\eta}
$$

which leads to the directivity-impedance relationship:

$$
D_{\max} = \frac{4\pi}{\Delta\Omega} = \frac{1}{c_n}\frac{\eta}{\pi R_{\text{peak}}}
$$

(17.3.8)

The normalization constant c_n is equal to unity for a half-wave dipole; for other antenna lengths, it may be computed numerically.

The MATLAB function `dipdir` calculates c_n, the directivity $D_{\max}$, the angle $\theta_{\max}$ at which the directivity is maximum (the angle $180 - \theta_{\max}$ also corresponds to $D_{\max}$), and the radiation resistance R_{peak}. It has usage:

```
[Rpeak,Dmax,thmax,cn] = dipdir(L)     % standing-wave dipole of length L
```
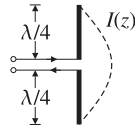
The radiation resistance is computed from Eq. (17.3.7) with the help of the sine and cosine integral functions $S_i(x)$ and $C_{\text{in}}(x)$, and $D_{\max}$ is computed from (17.3.8).

The table below shows some representative values, with the corresponding angular patterns shown in Fig. 17.4.2.

l/λ	R_{peak} (Ω)	$D_{\max}$	$D_{\max}$ (dB)	$\theta_{\max}$	c_n
0.50	73.08	1.64	2.15	90.00°	1.0000
0.75	185.68	1.88	2.75	90.00°	0.3431
1.00	198.95	2.41	3.82	90.00°	0.2500
1.25	106.46	3.28	5.16	90.00°	0.3431
1.50	105.42	2.23	3.48	42.57°	0.5109
1.75	229.94	2.37	3.75	50.94°	0.2200
2.00	259.45	2.53	4.03	57.42°	0.1828
2.25	143.48	3.07	4.87	62.28°	0.2723
2.50	120.68	3.06	4.86	32.22°	0.3249

17.4 Half-Wave Dipole

The *half-wave dipole* corresponding to $l = \lambda/2$, or $kl = \pi$, is one of the most common antennas. In this case, the current distribution along the antenna takes the form:

$$\boxed{I(z) = I\cos(kz)} \qquad \text{(half-wave dipole)} \qquad (17.4.1)$$

with $-\lambda/4 \leq z \leq \lambda/4$. The normalized gain is:

$$\boxed{g(\theta) = \frac{\cos^2(0.5\pi\cos\theta)}{\sin^2\theta}} \qquad \text{(half-wave dipole gain)} \qquad (17.4.2)$$

Note that the maximum does occur at $\theta = \pi/2$ and the normalization constant is $c_n = 1$. Fig. 17.4.1 shows the gain in absolute and dB units. The 3-dB or half-power circle intersects the gain at an angle of $\theta_{3dB} = 50.96^o$, which leads to a half-power beam width of HPBW $= 180^o - 2\theta_{3dB} = 78.08^o$, that is, somewhat narrower than the Hertzian dipole.
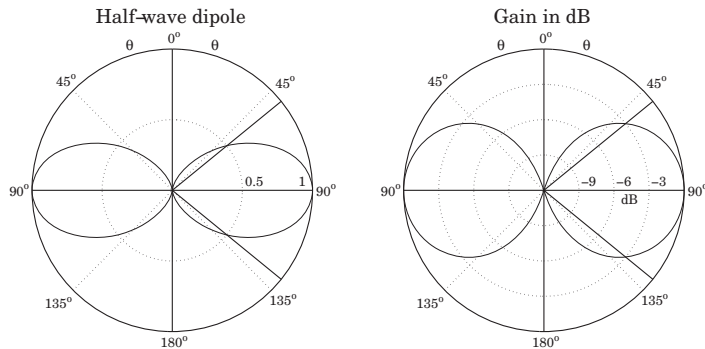

Fig. 17.4.1 Gain of half-wave dipole in absolute and dB units.

Because $\sin(kl/2) = 1$, $\sin(kl) = 0$, and $\cos(kl) = -1$, Eq. (17.3.7) reduces to:

$$R_{in} = R_{peak} = \frac{\eta}{4\pi} C_{in}(2kl) = \frac{\eta}{4\pi} C_{in}(2\pi) = 73.0790 \text{ ohm}$$

The directivity is found from (17.3.8) with $c_n = 1$:

$$D_{max} = \frac{\eta}{\pi R_{peak}} = 1.64 \equiv 2.15 \text{ dB}$$

In practice, the value $R_{in} = 73$ ohm can be matched easily to the characteristic impedance of the feed line. For arbitrary values of the length l, the following example MATLAB code used to calculate the gain function $g(\theta)$, as well as the constant c_n and the beam solid angle, is as follows:

```
N = 200;                                      % divide [0,pi] in N angle bins
dth = pi / N;                                 % bin width
th = (1:N-1) * dth;                           % excludes th=0
g = ((cos(pi*L*cos(th)) - cos(pi*L)) ./ sin(th)).^2;
th = [0, th];                                 % N equally-spaced angles in [0,pi]
g = [0, g];                                   % avoids division by 0
cn = 1 / max(g);
g = cn * g;                                    % normalized to unity maximum
Om = 2 * pi * sum(g .* sin(th)) * dth;        % beam solid angle
```

where the beam solid angle is computed by the approximation to the integral:

$$\Delta\Omega = 2\pi \int_0^\pi g(\theta)\sin\theta \, d\theta \simeq 2\pi \sum_{i=0}^{N-1} g(\theta_i)\sin\theta_i \, \Delta\theta$$

where $\Delta\theta = \pi/N$ and $\theta_i = i\Delta\theta$, $i = 0, 1, \ldots, N-1$. These operations are carried out by the functions `dipole` and `dmax`. For example, the right graph in Fig. 17.4.1 and D_{max} and $\Delta\Omega$ were generated by the MATLAB code:

```
[g, th, c] = dipole(0.5, 200);
dbp(th, g, 45, 12);
[D, Omega] = dmax(th, g);
```

Gauss-Legendre quadrature integration also produces accurate results. For example, assuming the normalization constant c_n is known, the following code fragment integrates the gain function (17.3.3) to compute the beam solid angle:

```
G = inline('(cos(pi*L*cos(th)) - cos(pi*L)).^2./sin(th).^2', 'L','th');

[w,th] = quadrs([0,pi/2,pi],32);              % use 32 points in the subintervals [0, π/2] and [π/2, π]
DOm = cn * 2*pi* w'*(G(L,th).*sin(th));       % find ΔΩ = 7.6581 for L = 0.5
```

Fig. 17.4.2 shows the gains of a variety of dipoles of different lengths. The corresponding directivities are indicated on each plot.

17.5 Monopole Antennas

A monopole antenna is half of a dipole antenna placed on top of a ground plane, as shown in Fig. 17.5.1. Assuming the plane is infinite and perfectly conducting, the monopole antenna will be equivalent to a dipole whose lower half is the *image* of the upper half.

Thus, the radiation pattern (in the upper hemisphere) will be identical to that of a dipole. Because the fields are radiated only in the upper hemisphere, the total radiated power will be half that of a dipole, and hence the corresponding radiation resistance will also be halved:

$$P_{monopole} = \frac{1}{2} P_{dipole}, \qquad R_{monopole} = \frac{1}{2} R_{dipole}$$

Similarly, the directivity doubles because the isotropic radiation intensity in the denominator of Eq. (16.2.2) becomes half its dipole value:
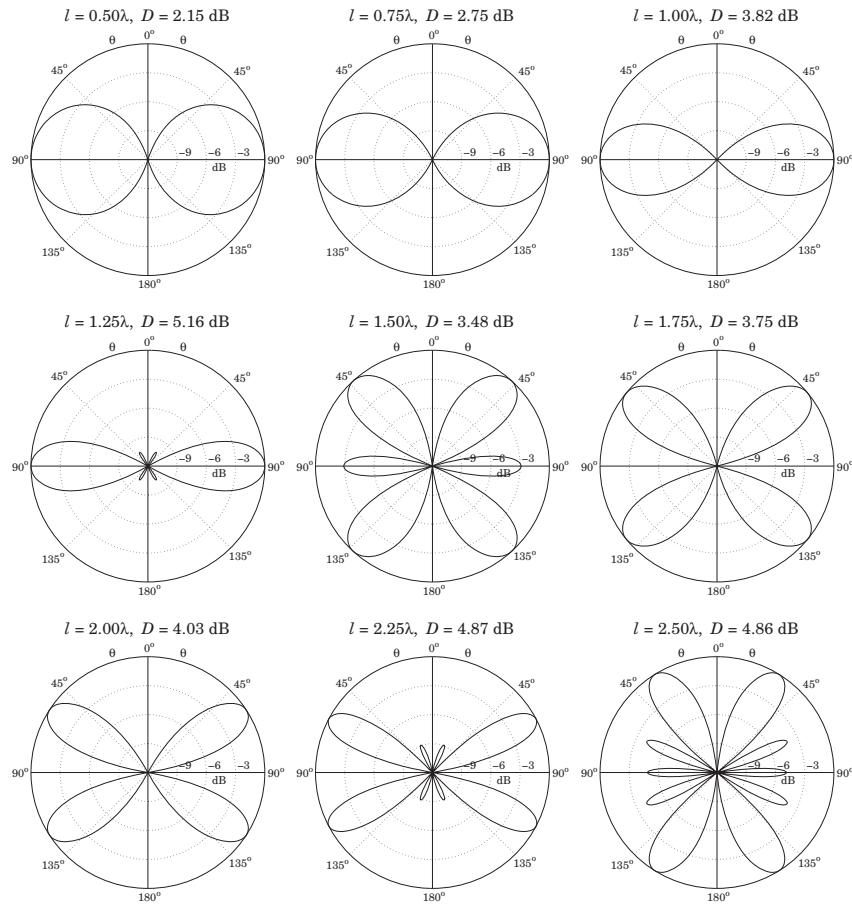
$$D_{monopole} = 2D_{dipole}$$

Fig. 17.4.2 Standing-wave dipole antenna patterns and directivities.

The *quarter-wave monopole* antenna whose length is $\lambda/4$ is perhaps the most widely used antenna. For AM transmitting antennas operating in the 300 m or 1 MHz band, the antenna height will be large, $\lambda/4 = 75$ m, requiring special supporting cables.

In mobile applications in the 30 cm or 1 GHz band, the antenna length will be fairly small, $\lambda/4 = 7.5$ cm. The roof of a car plays the role of the conducting plane in this case.

We note also in Fig. 17.4.2 that the $l = 1.25\lambda = 10\lambda/8$ dipole has the largest gain. It can be used as a monopole in mobile applications requiring higher gains. Such antennas are called 5/8-*wave monopoles* because their length is $l/2 = 5\lambda/8$.
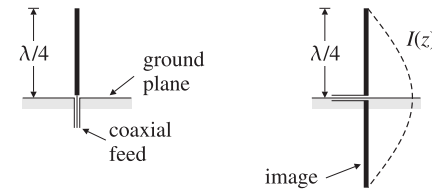
Fig. 17.5.1 Quarter-wave monopole above ground plane and the equivalent half-wave dipole.

17.6 Traveling-Wave Antennas

The standing-wave antenna current may be thought of as the linear superposition of a forward and a backward moving current. For example, the half-wave dipole current can be written in the form:

$$I(z)= I\cos(kz)= \frac{I}{2}(e^{-jkz} + e^{jkz})$$

The backward-moving component may be eliminated by terminating the linear antenna at an appropriate matched load resistance, as shown in Fig. 17.6.1. The resulting antenna is called a *traveling-wave* antenna or a *Beverage* antenna. The current along its length has the form:

$$I(z)= Ie^{-jkz}, \qquad 0 \le z \le l \tag{17.6.1}$$

The corresponding radiation vector becomes:

$$\mathbf{F} = \hat{\mathbf{z}} \int_0^l Ie^{-jkz'} e^{jk\cos\theta\, z'} dz' = \hat{\mathbf{z}}\,\frac{I}{jk}\,\frac{1 - e^{-jkl(1-\cos\theta)}}{1 - \cos\theta} \tag{17.6.2}$$

The transverse θ-component is:

$$F_\theta(\theta)= -F_z(\theta)\sin\theta = -\frac{I}{jk}\,\sin\theta\,\frac{1 - e^{-2\pi jL(1-\cos\theta)}}{1 - \cos\theta} \equiv -\frac{I}{jk}\,F(\theta) \tag{17.6.3}$$

where as before, $L = l/\lambda$ and $kl = 2\pi l/\lambda = 2\pi L$. The radiation intensity, given by Eq. (16.1.4) or (17.1.7), becomes now:

$$U(\theta)= \frac{\eta|I|^2}{32\pi^2}\,|F(\theta)|^2 = \frac{\eta|I|^2}{8\pi^2}\left|\frac{\sin\theta\,\sin(\pi L(1-\cos\theta))}{1 - \cos\theta}\right|^2 \tag{17.6.4}$$
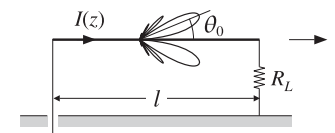

Fig. 17.6.1 Traveling-wave antenna with matched termination.

Therefore, the normalized power gain will be:

$$g(\theta) = c_n \left| \frac{\sin\theta \, \sin(\pi L(1 - \cos\theta))}{1 - \cos\theta} \right|^2 \qquad (17.6.5)$$

where c_n is a normalization constant. Fig. 17.6.2 shows the power gains and directivities for the cases $l = 5\lambda$ and $l = 10\lambda$, or $L = 5$ and $L = 10$.
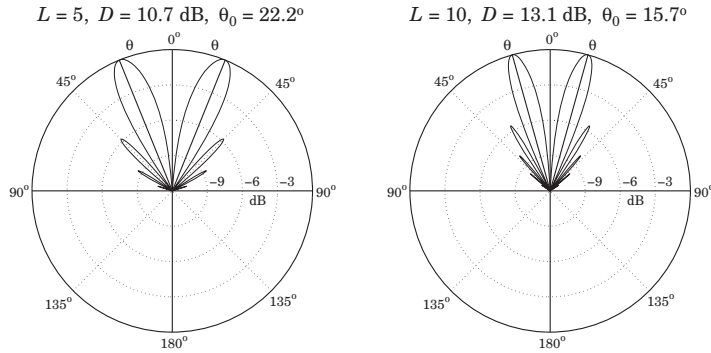

Fig. 17.6.2 Traveling-wave antenna gain examples.

The MATLAB function `traveling` calculates the gain (17.6.5). For example, the left graph in Fig. 17.6.2 was generated by the MATLAB code:

```
[g, th, c, th0] = traveling(5, 400);
dbp(th, g, 45, 12);
addray(90-th0,'-'); addray(90+th0,'-');
```

The longer the length l, the more the main lobes tilt towards the traveling direction of the antenna. The main lobes occur approximately at the polar angle (in radians) [5–7]:

$$\boxed{\theta_0 = \arccos\left(1 - \frac{0.371\lambda}{l}\right) = \arccos\left(1 - \frac{0.371}{L}\right)} \qquad (17.6.6)$$

For the two examples of Fig. 17.6.2, this expression gives for $L = 5$ and $L = 10$, $\theta_0 = 22.2°$ and $\theta_0 = 15.7°$. As L increases, the angle θ_0 tends to zero.

There are other antenna structures that act as traveling-wave antennas, as shown in Fig. 17.6.3. For example, a waveguide with a long slit along its length will radiate continuously along the slit. Another example is a corrugated conducting surface along which a surface wave travels and gets radiated when it reaches the discontinuity at the end of the structure.

In all of these examples, the radiation pattern has an angular dependence similar to that of a linear antenna with a traveling-wave current of the form:

$$I(z) = I e^{-j\beta z} = I e^{-jpkz}, \qquad 0 \le z \le l \qquad (17.6.7)$$
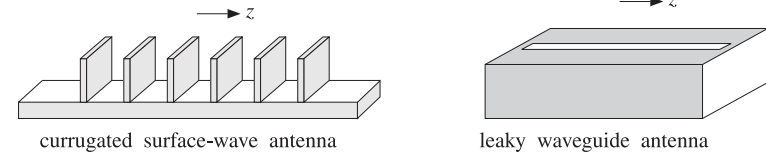
Fig. 17.6.3 Surface-wave and leaky-wave antennas.

where β is the wavenumber along the guiding structure and $p = \beta/k = c/v_{\text{phase}}$ is the ratio of the speed of light in vacuum to the phase velocity along the guide. The corresponding radiation power pattern will now have the form:

$$g(\theta) = c_n \left| \frac{\sin\theta \, \sin(\pi L(p - \cos\theta))}{p - \cos\theta} \right|^2 \qquad (17.6.8)$$

For long lengths L (and for $p < 1$), it peaks along the direction $\theta_0 = \arccos(p)$. Note that p can take the values: (a) $p > 1$ (slow waves), as in the case of the corrugated plane structure or the case of a Beverage antenna wrapped in a dielectric, (b) $p < 1$ (fast waves), as in the case of the leaky waveguide, where $p = \sqrt{1 - \omega_c^2/\omega^2}$, and (c) $p = 1$, for the Beverage antenna.

17.7 Vee and Rhombic Antennas

A vee antenna consists of two traveling-wave antennas forming an angle 2α with each other, as shown in Fig. 17.7.1. It may be constructed by opening up the matched ends of a transmission line at an angle of 2α (each of the terminating resistances is $R_L/2$ for a total of R_L.)
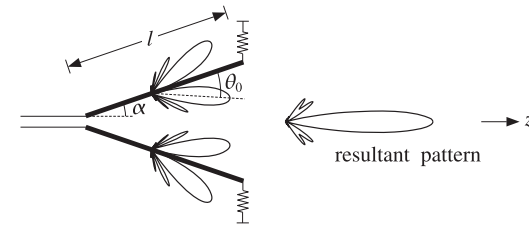

Fig. 17.7.1 Traveling-wave vee antenna with $l = 5\lambda$, $\theta_0 = 22.2°$, and $\alpha = 0.85\theta_0 = 18.9°$.

By choosing the angle α to be approximately equal to the main lobe angle θ_0 of Eq. (17.6.6), the two inner main lobes align with each other along the middle direction and produce a stronger main lobe, thus increasing the directivity of the antenna. The outer main lobes will also be present, but smaller.

The optimum angle α of the arms of the vee depends on the length l and is related to main lobe angle θ_0 via $\alpha = a\theta_0$, where the factor a typically falls in the range

$a = 0.80$-1.00. Figure 17.7.2 shows the optimum angle factor a that corresponds to maximum directivity (in the plane of the vee) as a function of the length l.
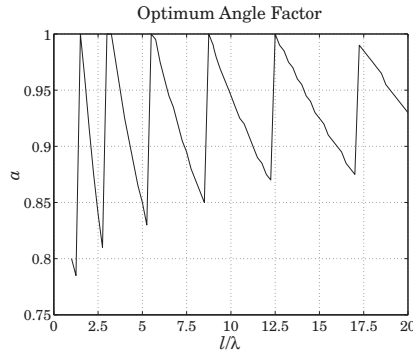

Fig. 17.7.2   Optimum angle factor as a function of antenna length.

Figure 17.7.3 shows the actual power patterns for the cases $l = 5\lambda$ and $l = 10\lambda$. The main lobe angles were $\theta_0 = 22.2°$ and $\theta_0 = 15.7°$. The optimum vee angles were found to be approximately (see Fig. 17.7.2), $\alpha = 0.85\theta_0 = 18.9°$ and $\alpha = 0.95\theta_0 = 14.9°$, in the two cases.
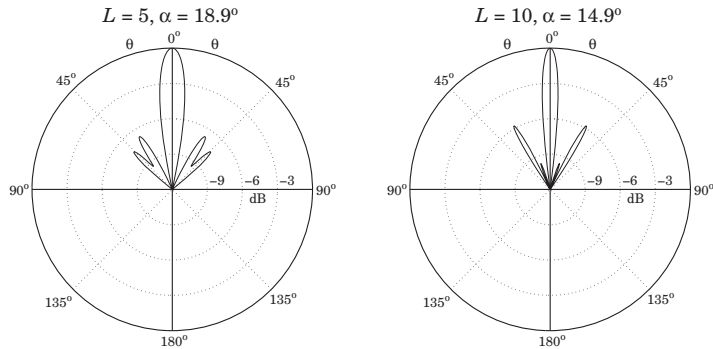

Fig. 17.7.3   Traveling-wave vee antenna gains in dB.

The combined radiation pattern can be obtained with the help of Fig. 17.7.4. Let $\hat{\mathbf{z}}_1$ and $\hat{\mathbf{z}}_2$ be the two unit vectors along the two arms of the vee, and let θ_1, θ_2 be the two polar angles of the observation point P with respect to the directions $\hat{\mathbf{z}}_1, \hat{\mathbf{z}}_2$. The assumed currents along the two arms have opposite amplitudes and are:

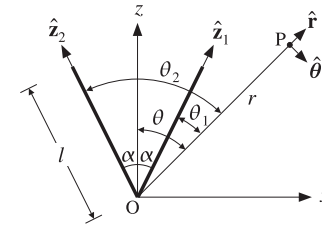$$I_1(z_1) = Ie^{-jkz_1}, \qquad I_2(z_2) = -Ie^{-jkz_2}, \qquad \text{for} \quad 0 \le z_1, z_2 \le l$$

Fig. 17.7.4   Radiation vectors of traveling-wave vee antenna.

Applying the result of Eq. (17.6.2), the radiation vectors of the two arms will be:

$$\mathbf{F}_1 = \hat{\mathbf{z}}_1 \int_0^l Ie^{-jkz_1'} e^{jk\cos\theta_1 z_1'} dz_1' = \hat{\mathbf{z}}_1 \frac{I}{jk} \frac{1 - e^{-jkl(1-\cos\theta_1)}}{1 - \cos\theta_1}$$

$$\mathbf{F}_2 = -\hat{\mathbf{z}}_2 \int_0^l Ie^{-jkz_2'} e^{jk\cos\theta_2 z_2'} dz_2' = -\hat{\mathbf{z}}_2 \frac{I}{jk} \frac{1 - e^{-jkl(1-\cos\theta_2)}}{1 - \cos\theta_2}$$

Therefore, the θ-components will be as in Eq. (17.6.3):

$$F_{1\theta} = -\frac{I}{jk} F(\theta_1), \qquad F_{2\theta} = \frac{I}{jk} F(\theta_2)$$

where the function $F(\theta)$ was defined in Eq. (17.6.3). From Fig. 17.7.4, we may express θ_1, θ_2 in terms of the polar angle θ with respect to the z-axis as:

$$\theta_1 = \theta - \alpha, \qquad \theta_2 = \theta + \alpha$$

Adding the θ-components, we obtain the resultant:

$$F_\theta = F_{1\theta} + F_{2\theta} = \frac{I}{jk}\big[F(\theta_2) - F(\theta_1)\big] = \frac{I}{jk}\big[F(\theta + \alpha) - F(\theta - \alpha)\big]$$

Thus, the radiation intensity will be:

$$U(\theta) = \frac{\eta k^2}{32\pi^2}|F_\theta(\theta)|^2 = \frac{\eta|I|^2}{32\pi^2}\big|F(\theta + \alpha) - F(\theta - \alpha)\big|^2$$

and the normalized power pattern:

$$g(\theta) = c_n\big|F(\theta + \alpha) - F(\theta - \alpha)\big|^2 \tag{17.7.1}$$

This is the gain plotted in Fig. 17.7.3 and can be computed by the MATLAB function **vee**. Finally, we consider briefly a rhombic antenna made up of two concatenated vee antennas, as shown in Fig. 17.7.5. Now the two inner main lobes of the first vee (lobes a, b) and the two outer lobes of the second vee (lobes c, d) align with each other, thus increasing the directivity of the antenna system.

The radiation vectors $\mathbf{F}_3$ and $\mathbf{F}_4$ of arms 3 and 4 may be obtained by noting that these arms are the translations of arms 1 and 2, and therefore, the radiation vectors are changed by the appropriate translational phase shift factors, as discussed in Sec. 22.2.
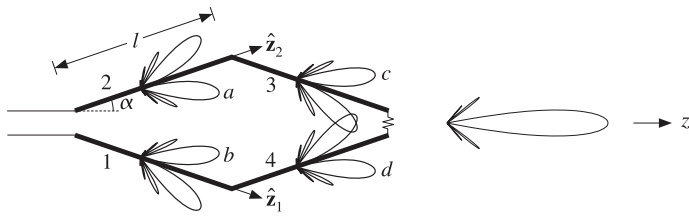
Fig. 17.7.5 Traveling-wave rhombic antenna.

Arm-3 is the translation of arm-1 by the vector $\mathbf{d}_2 = l\,\hat{\mathbf{z}}_2$ and arm-4 is the translation of arm-2 by the vector $\mathbf{d}_1 = l\,\hat{\mathbf{z}}_1$. Thus, the corresponding radiation vectors will be:

$$F_3 = -e^{j\mathbf{k}\cdot\mathbf{d}_2}F_1\,, \qquad F_4 = -e^{j\mathbf{k}\cdot\mathbf{d}_1}F_2 \qquad (17.7.2)$$

where the negative signs arise because the currents in those arms have opposite signs with their parallel counterparts. The phase shift factors are:

$$e^{j\mathbf{k}\cdot\mathbf{d}_2} = e^{jkl\hat{\mathbf{r}}\cdot\hat{\mathbf{z}}_2} = e^{jkl\cos\theta_2}\,, \qquad e^{j\mathbf{k}\cdot\mathbf{d}_1} = e^{jkl\hat{\mathbf{r}}\cdot\hat{\mathbf{z}}_1} = e^{jkl\cos\theta_1}$$

It follows that the θ-components of F_3 and F_4 are:

$$F_{3\theta} = -e^{jkl\cos\theta_2}F_{1\theta} = \frac{I}{jk}e^{jkl\cos\theta_2}F(\theta_1)$$

$$F_{4\theta} = -e^{jkl\cos\theta_1}F_{2\theta} = -\frac{I}{jk}e^{jkl\cos\theta_1}F(\theta_2)$$

Thus, the resultant θ-component will be:

$$F_\theta = F_{1\theta} + F_{2\theta} + F_{3\theta} + F_{4\theta} = \frac{I}{jk}\left[F(\theta_2) - F(\theta_1) + e^{jkl\cos\theta_2}F(\theta_1) - e^{jkl\cos\theta_1}F(\theta_2)\right]$$

The corresponding normalized power pattern will be:

$$g(\theta) = c_n\left|F(\theta+\alpha) - F(\theta-\alpha) + e^{jkl\cos(\theta+\alpha)}F(\theta-\alpha) - e^{jkl\cos(\theta-\alpha)}F(\theta+\alpha)\right|^2$$

Figure 17.7.6 shows the power gain $g(\theta)$ for the cases $L = 5$ and $L = 10$. The optimum vee angle in both cases was found to be $\alpha = \theta_0$, that is, $\alpha = 22.2°$ and $\alpha = 15.7°$. The function rhombic may be used to evaluate this expression.

17.8 Loop Antennas

Figure 17.8.1 shows a circular and a square loop antenna. The feed points are not shown. The main oversimplifying assumption here is that the current is constant around the loop. We will mainly consider the case when the dimension of the loop (e.g., its circumference) is small relative to the wavelength.
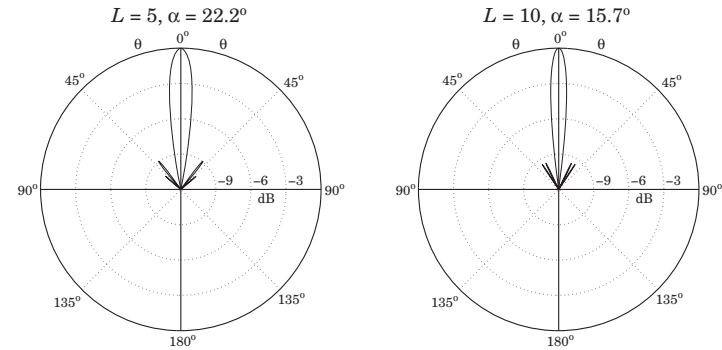
Fig. 17.7.6 Rhombic antenna gains in dB.

For such small loops, the radiation pattern turns out to be *independent* of the shape of the loop and the radiation vector takes the simple form:

$$F = j\,\mathbf{m}\times\mathbf{k} \qquad (17.8.1)$$

where $\mathbf{m}$ is the loop's magnetic moment defined with respect to Fig. 17.8.1 as follows:

$$\mathbf{m} = \hat{\mathbf{z}}\,IS\,, \qquad \text{(magnetic moment)} \qquad (17.8.2)$$

where S is the area of the loop. Writing $\mathbf{k} = k\,\hat{\mathbf{r}}$ and noting that $\hat{\mathbf{z}}\times\hat{\mathbf{r}} = \hat{\boldsymbol{\phi}}\sin\theta$, we have:

$$F = j\,\mathbf{m}\times\mathbf{k} = jmk\sin\theta\,\hat{\boldsymbol{\phi}} \equiv F_\phi(\theta)\hat{\boldsymbol{\phi}} \qquad (17.8.3)$$

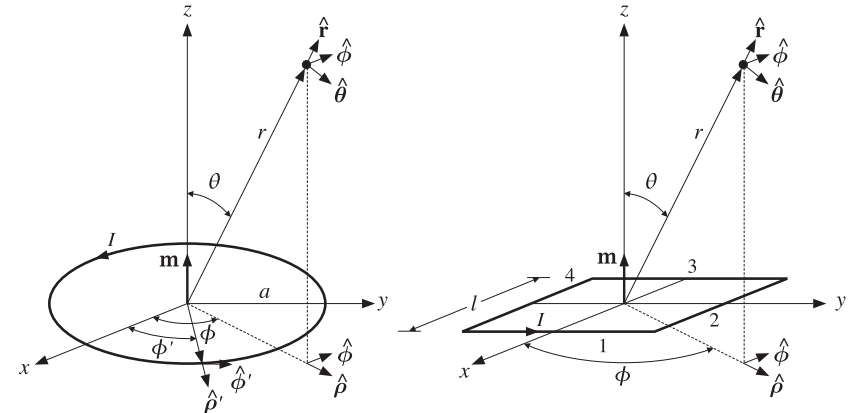**Fig. 17.8.1** Circular and square loop antennas.

Thus, F is fully transverse to $\hat{\mathbf{r}}$, so that $F_\perp = F$. It follows from Eq. (15.10.4) that the produced radiation fields will be:

$$E = \hat{\boldsymbol{\phi}} E_\phi = -jk\eta \frac{e^{-jkr}}{4\pi r} F_\phi \hat{\boldsymbol{\phi}} = \eta m k^2 \sin\theta \frac{e^{-jkr}}{4\pi r} \hat{\boldsymbol{\phi}}$$

$$H = \hat{\boldsymbol{\theta}} H_\theta = jk \frac{e^{-jkr}}{4\pi r} F_\phi \hat{\boldsymbol{\theta}} = -mk^2 \sin\theta \frac{e^{-jkr}}{4\pi r} \hat{\boldsymbol{\theta}}$$

(17.8.4)

The radiation intensity of Eq. (16.1.4) is in this case:

$$\boxed{U(\theta, \phi) = \frac{\eta k^2}{32\pi^2} |F_\phi|^2 = \frac{\eta k^4 |m|^2}{32\pi^2} \sin^2\theta} \qquad \text{(loop intensity)} \qquad (17.8.5)$$

Thus, it has the same $\sin^2\theta$ angular dependence, normalized power gain, and directivity as the Hertzian dipole. We may call such small loop antennas "Hertzian loops", referring to their infinitesimal size. The total radiated power can be computed as in Sec. 17.2. We have:

$$P_{\text{rad}} = U_{\max} \Delta\Omega = \frac{\eta k^4 |m|^2}{32\pi^2} \frac{8\pi}{3} = \frac{\eta k^4 |m|^2}{12\pi}$$

Replacing m by IS, we may obtain the loop's radiation resistance from the definition:

$$P_{\text{rad}} = \frac{1}{2} R_{\text{rad}} |I|^2 = \frac{\eta k^4 |IS|^2}{12\pi} \qquad \Rightarrow \qquad R_{\text{rad}} = \frac{\eta k^4 S^2}{6\pi}$$

Comparing Eq. (17.8.4) to the Hertzian dipole, the loop's electric field is in the ϕ-direction, whereas the Hertzian dipole's is in the θ-direction. The relative amplitudes of the electric fields are:

$$\frac{E_\theta^{\text{dipole}}}{E_\phi^{\text{loop}}} = j \frac{Il}{mk}$$

If we choose $Il = mk$, then the electric fields are off by a 90°-degree phase. If such a Hertzian dipole and loop are placed at the origin, the produced net electric field will be *circularly* polarized. We note finally that the loop may have several turns, thus increasing its radiation resistance and radiated power. For a loop with n turns, we must make the replacement $m \to nm$.

17.9 Circular Loops

Next, we consider the circular loop in more detail, and derive Eq. (17.8.3). Assuming an infinitely thin wire loop of radius a, the assumed current density can be expressed in cylindrical coordinates as in Eq. (17.1.3):

$$J(\mathbf{r}') = I \hat{\boldsymbol{\phi}}' \delta(\rho' - a) \delta(z')$$

The radiation vector will be:

$$F = \int_V J(\mathbf{r}') e^{j\mathbf{k}\cdot\mathbf{r}'} d^3\mathbf{r}' = \int I \hat{\boldsymbol{\phi}}' e^{j\mathbf{k}\cdot\mathbf{r}'} \delta(\rho' - a) \delta(z') \rho' d\rho' d\phi' dz' \qquad (17.9.1)$$

Using Eq. (15.8.2), we have:

$$\mathbf{k}\cdot\mathbf{r}' = k(\hat{\mathbf{z}}\cos\theta + \hat{\boldsymbol{\rho}}\sin\theta)\cdot(z'\hat{\mathbf{z}} + \rho'\hat{\boldsymbol{\rho}}')$$

$$= kz'\cos\theta + k\rho'\sin\theta(\hat{\boldsymbol{\rho}}'\cdot\hat{\boldsymbol{\rho}})$$

$$= kz'\cos\theta + k\rho'\sin\theta\cos(\phi' - \phi)$$

where we set $\hat{\boldsymbol{\rho}}'\cdot\hat{\boldsymbol{\rho}} = \cos(\phi' - \phi)$, as seen in Fig. 17.8.1. The integration in Eq. (17.9.1) confines $\mathbf{r}'$ to the xy-plane and sets $\rho' = a$ and $z' = 0$. Thus, we have in the integrand:

$$\mathbf{k}\cdot\mathbf{r}' = ka\sin\theta\cos(\phi' - \phi)$$

Then, the radiation vector (17.9.1) becomes:

$$F = Ia \int_0^{2\pi} \hat{\boldsymbol{\phi}}' e^{jka\sin\theta\cos(\phi'-\phi)} d\phi' \qquad (17.9.2)$$

We note in Fig. 17.8.1 that the unit vector $\hat{\boldsymbol{\phi}}'$ varies in direction with ϕ'. Therefore, it proves convenient to express it in terms of the unit vectors $\hat{\boldsymbol{\phi}}, \hat{\boldsymbol{\rho}}$ of the fixed observation point P. Resolving $\hat{\boldsymbol{\phi}}'$ into the directions $\hat{\boldsymbol{\phi}}, \hat{\boldsymbol{\rho}}$, we have:

$$\hat{\boldsymbol{\phi}}' = \hat{\boldsymbol{\phi}}\cos(\phi' - \phi) - \hat{\boldsymbol{\rho}}\sin(\phi' - \phi)$$

Changing integration variables from ϕ' to $\psi = \phi' - \phi$, we write Eq. (17.9.2) as:

$$F = Ia \int_0^{2\pi} (\hat{\boldsymbol{\phi}}\cos\psi - \hat{\boldsymbol{\rho}}\sin\psi) e^{jka\sin\theta\cos\psi} d\psi$$

The second term is odd in ψ and vanishes. Thus,

$$F = Ia\hat{\boldsymbol{\phi}} \int_0^{2\pi} \cos\psi e^{jka\sin\theta\cos\psi} d\psi \qquad (17.9.3)$$

Using the integral representation of the Bessel function $J_1(x)$,

$$J_1(x) = \frac{1}{2\pi j} \int_0^{2\pi} \cos\psi\, e^{jx\cos\psi} d\psi$$

we may replace the ψ-integral by $2\pi j J_1(ka\sin\theta)$ and write Eq. (17.9.3) as:

$$F = F_\phi \hat{\boldsymbol{\phi}} = 2\pi j Ia J_1(ka\sin\theta)\hat{\boldsymbol{\phi}} \qquad (17.9.4)$$

This gives the radiation vector for any loop radius. If the loop is electrically small, that is, $ka \ll 1$, we may use the first-order approximation $J_1(x) \simeq x/2$, to get

$$F = F_\phi \hat{\boldsymbol{\phi}} = 2\pi j Ia \frac{1}{2} ka\sin\theta\, \hat{\boldsymbol{\phi}} = jI\pi a^2 k\sin\theta\, \hat{\boldsymbol{\phi}} \qquad (17.9.5)$$

which agrees with Eq. (17.8.3), with $m = IS = I\pi a^2$.

17.10 Square Loops

The square loop of Fig. 17.8.1 may be thought of as four separate linear antennas representing the four sides. Assuming that each side is a Hertzian dipole and that the sides are at distances $\pm l/2$ from the origin, we can write the current densities of the sides 1, 2, 3, 4 as follows:

$$J_1(\mathbf{r}) = \hat{\mathbf{y}} Il\,\delta(x - l/2)\,\delta(y)\,\delta(z)$$

$$J_2(\mathbf{r}) = -\hat{\mathbf{x}} Il\,\delta(x)\,\delta(y - l/2)\,\delta(z)$$

$$J_3(\mathbf{r}) = -\hat{\mathbf{y}} Il\,\delta(x + l/2)\,\delta(y)\,\delta(z)$$

$$J_4(\mathbf{r}) = \hat{\mathbf{x}} Il\,\delta(x)\,\delta(y + l/2)\,\delta(z)$$

The currents on the parallel sides 1 and 3 combine to give:

$$J_1(\mathbf{r}) + J_3(\mathbf{r}) = -Il^2\,\hat{\mathbf{y}}\left[\frac{\delta(x + l/2) - \delta(x - l/2)}{l}\right]\delta(y)\,\delta(z)$$

where we multiplied and divided by a factor of l. In the limit of small l, we may replace the quantity in the bracket by the derivative $\delta'(x)$ of the delta function $\delta(x)$:

$$J_1(\mathbf{r}) + J_3(\mathbf{r}) = -Il^2\,\hat{\mathbf{y}}\,\delta'(x)\,\delta(y)\,\delta(z)$$

Similarly, we find for sides 2 and 4:

$$J_2(\mathbf{r}) + J_4(\mathbf{r}) = Il^2\,\hat{\mathbf{x}}\,\delta(x)\,\delta'(y)\,\delta(z)$$

Thus, the net current density of all sides is:

$$J(\mathbf{r}) = Il^2\left[\hat{\mathbf{x}}\,\delta(x)\,\delta'(y) - \hat{\mathbf{y}}\,\delta'(x)\,\delta(y)\right]\delta(z) \tag{17.10.1}$$

The corresponding radiation vector will be:

$$\mathbf{F} = Il^2\int\left[\hat{\mathbf{x}}\,\delta(x')\,\delta'(y') - \hat{\mathbf{y}}\,\delta'(x')\,\delta(y')\right]\delta(z')e^{j(k_xx' + k_yy' + k_zz')}dx'\,dy'\,dz'$$

The delta-function integrations can be done easily yielding:

$$\mathbf{F} = Il^2(-jk_y\hat{\mathbf{x}} + jk_x\hat{\mathbf{y}})$$

Using Eq. (17.1.4), we obtain

$$\mathbf{F} = jIl^2k\sin\theta\,(-\hat{\mathbf{x}}\sin\phi + \hat{\mathbf{y}}\cos\phi) = jIl^2k\sin\theta\,\hat{\boldsymbol{\phi}} \tag{17.10.2}$$

which agrees with Eq. (17.8.3), with $m = IS = Il^2$.

17.11 Dipole and Quadrupole Radiation

The radiation vector $\mathbf{F}$ of a current/charge distribution can be evaluated approximately by expanding the exponential $e^{j\mathbf{k}\cdot\mathbf{r}'}$ to successive powers of $\mathbf{k}$:

$$\mathbf{F} = \int_V J(\mathbf{r}')e^{j\mathbf{k}\cdot\mathbf{r}'}d^3\mathbf{r}' = \int_V\left[1 + j\mathbf{k}\cdot\mathbf{r}' + \frac{1}{2!}(j\mathbf{k}\cdot\mathbf{r}')^2 + \cdots\right]J(\mathbf{r}')d^3\mathbf{r}'$$

$$= \underbrace{\int_V J(\mathbf{r}')d^3\mathbf{r}'}_{\text{elec. dipole}} + \underbrace{\int_V j(\mathbf{k}\cdot\mathbf{r}')J(\mathbf{r}')d^3\mathbf{r}'}_{\text{magn. dipole \& elec. quadrupole}} + \cdots \tag{17.11.1}$$

The first term is the *electric dipole* radiation term and corresponds to the Hertzian dipole antenna. The second term incorporates both the *magnetic dipole* (corresponding to a Hertzian loop antenna) and the *electric quadrupole* terms.

Higher multipoles arise from the higher-order terms in the above expansion. A systematic discussion of all multipole radiation terms requires the use of spherical harmonics.

Keeping only a few terms in the above expansion is a good approximation to $\mathbf{F}$ provided $kr' \ll 1$, or $l \ll \lambda$, where l is the typical dimension of the current source. In general, any radiating system will emit radiation of various multipole types.

The *electric dipole* and *electric quadrupole moments* of a charge distribution are defined in terms of the following first- and second-order moments of the charge density:

$$\mathbf{p} = \int_V \mathbf{r}'\rho(\mathbf{r}')\,d^3\mathbf{r}' \qquad \text{(electric dipole moment)} \tag{17.11.2}$$

$$D_{ij} = \int_V r_i'r_j'\rho(\mathbf{r}')\,d^3\mathbf{r}' \qquad \text{(electric quadrupole moment)} \tag{17.11.3}$$

The identity of Problem 15.2 is useful here in manipulating the successive expansion terms of $\mathbf{F}$. Applying the identity with the two choices: $g(\mathbf{r}') = r_i'$ and $g(\mathbf{r}') = r_i'r_j'$, we obtain the relationships:

$$\int_V J_i\,d^3\mathbf{r}' = j\omega\int_V r_i'\rho(\mathbf{r}')\,d^3\mathbf{r}' = j\omega p_i$$

$$\int_V (r_i'J_j + r_j'J_i)\,d^3\mathbf{r}' = j\omega\int_V r_i'r_j'\rho(\mathbf{r}')\,d^3\mathbf{r}' = j\omega D_{ij} \tag{17.11.4}$$

Thus, the lowest-order term in Eq. (17.11.1) is the electric dipole:

$$\int_V J(\mathbf{r}')\,d^3\mathbf{r}' = j\omega\,\mathbf{p} = \mathbf{F}_{\text{el}}$$

In the second term of Eq. (17.11.1), we may apply the vectorial identity:

$$(\mathbf{k}\cdot\mathbf{r}')J = \frac{1}{2}(\mathbf{r}'\times J)\times\mathbf{k} + \frac{1}{2}\left[(\mathbf{k}\cdot\mathbf{r}')J + (\mathbf{k}\cdot J)\mathbf{r}'\right]$$

and in integrated form:

$$\int_V (\mathbf{k}\cdot\mathbf{r}')J\,d^3\mathbf{r}' = \frac{1}{2}\int_V (\mathbf{r}'\times J)\times\mathbf{k}\,d^3\mathbf{r}' + \frac{1}{2}\int_V\left[(\mathbf{k}\cdot\mathbf{r}')J + (\mathbf{k}\cdot J)\mathbf{r}'\right]d^3\mathbf{r}' \tag{17.11.5}$$

The *magnetic moment* of a current distribution is defined in general by

$$\mathbf{m} = \frac{1}{2} \int_V \mathbf{r}' \times \mathbf{J}(\mathbf{r}')\, d^3\mathbf{r}' \qquad \text{(magnetic moment)} \tag{17.11.6}$$

Therefore, the first term in Eq. (17.11.5) may be written as $\mathbf{m} \times \mathbf{k}$. With the help of the second identity of Eq. (17.11.4), the last term of (17.11.5) may be written in terms of the quadrupole matrix D acting on the vector $\mathbf{k}$. We have then for the second term in the expansion (17.11.1):

$$\int_V j(\mathbf{k} \cdot \mathbf{r}')\mathbf{J} d^3\mathbf{r}' = j\mathbf{m} \times \mathbf{k} - \frac{1}{2}\omega D\mathbf{k} = \mathbf{F}_{\text{mag}} + \mathbf{F}_{\text{quad}} \tag{17.11.7}$$

Thus, the three lowest-order terms of $\mathbf{F}$ are:

$$\boxed{\mathbf{F} = \mathbf{F}_{\text{el}} + \mathbf{F}_{\text{mag}} + \mathbf{F}_{\text{quad}} = j\omega\,\mathbf{p} + j\mathbf{m} \times \mathbf{k} - \frac{1}{2}\omega D\mathbf{k}} \tag{17.11.8}$$

We briefly discuss each term. For a Hertzian dipole antenna with $\mathbf{J}(\mathbf{r}') = \hat{\mathbf{z}} Il\,\delta^3(\mathbf{r}')$, only the first term of (17.11.8) is non-zero and is the same as that of Sec. 17.2:

$$\mathbf{F}_{\text{el}} = \int_V \mathbf{J}(\mathbf{r}')\, d^3\mathbf{r}' = \hat{\mathbf{z}} Il = j\omega\,\mathbf{p}$$

The relationship $Il = j\omega p$ may be understood by thinking of the Hertzian dipole as two opposite time-varying charges $\pm q$ separated by a distance l (along the z-direction), so that $p = ql$. It follows that $j\omega p = \dot{p} = \dot{q}l = Il$.

The result $p = ql$ may also be applied to the case of an accelerated charge. Now q is constant but l varies with time. We have $\dot{p} = q\dot{l} = qv$ and $\ddot{p} = q\dot{v} = qa$, where a is the acceleration $a = \dot{v}$. For harmonic time dependence, we have $(j\omega)^2 p = qa$. The total radiated power from a dipole was obtained in Eq. (17.2.2). Setting $k^2|Il|^2 = k^2|qv|^2 = q^2\omega^2|v|^2/c^2 = q^2|a|^2/c^2$, we can rewrite Eq. (17.2.2) in the form:

$$P = \frac{\eta q^2|a|^2}{12\pi c^2} = \frac{\eta q^2 a_{\text{rms}}^2}{6\pi c^2}$$

where $a_{\text{rms}} = |a|/\sqrt{2}$ is the rms value of the acceleration. This is Larmor's classical expression for the radiated power from a nonrelativistic accelerated charge.

For a Hertzian loop, only the magnetic moment term is present in $\mathbf{F}$. We may verify the result that $\mathbf{m} = \hat{\mathbf{z}} IS$ using the definition (17.11.6). Indeed, for a circular loop:

$$\mathbf{m} = \frac{1}{2} \int \mathbf{r}' \times [I\hat{\boldsymbol{\phi}}'\,\delta(\rho' - a)\,\delta(z')]\rho'd\rho'\,d\phi'\,dz'$$

The integrations over z' and ρ' force $z' = 0$ and $\rho' = a$, and therefore, $\mathbf{r}' = a\hat{\boldsymbol{\rho}}'$. Noting that $\hat{\boldsymbol{\rho}}' \times \hat{\boldsymbol{\phi}}' = \hat{\mathbf{z}}$ and that the ϕ'-integration contributes a factor of 2π, we obtain:

$$\mathbf{m} = \frac{1}{2} a\hat{\boldsymbol{\rho}}' \times \hat{\boldsymbol{\phi}}'\, Ia\, 2\pi = \hat{\mathbf{z}} I(\pi a^2)$$

Similarly, inserting Eq. (17.10.1) into (17.11.6), we find for the square loop:

$$\mathbf{m} = \frac{1}{2} \int (x\hat{\mathbf{x}} + y\hat{\mathbf{y}} + z\hat{\mathbf{z}}) \times [Il^2(\hat{\mathbf{x}}\,\delta(x)\,\delta'(y) - \hat{\mathbf{y}}\,\delta'(x)\,\delta(y))\delta(z)]dx\,dy\,dz = \hat{\mathbf{z}} Il^2$$

For the electric quadrupole term, the matrix D is sometimes replaced by its *traceless* version defined by

$$Q_{ij} = 3D_{ij} - \delta_{ij}\text{tr}(D) = \int_V (3r_i'r_j' - \delta_{ij}\,\mathbf{r}' \cdot \mathbf{r}')\rho(\mathbf{r}')\,d^3\mathbf{r}' \quad \Rightarrow \quad Q = 3D - I\,\text{tr}(D)$$

so that $\text{tr}(Q) = 0$. In this case, the vector $D\mathbf{k}$ may be expressed as

$$D\mathbf{k} = \frac{1}{3} Q\mathbf{k} + \frac{1}{3}\text{tr}(D)\,\mathbf{k}$$

The second term may be ignored because it does not contribute to the radiation fields, which depend only on the part of $\mathbf{F}$ transverse to $\mathbf{k}$. Thus, without loss of generality we may also write:

$$\mathbf{F} = j\omega\,\mathbf{p} + j\mathbf{m} \times \mathbf{k} - \frac{1}{6}\omega Q\mathbf{k}$$

The electric and magnetic dipoles have angular gain patterns that are identical to the Hertzian dipole and Hertzian loop antennas, that is, $\sin^2\theta$. The quadrupole term, on the other hand, can have a complicated angular pattern as can be seen by expressing the vector $Q\mathbf{k} = kQ\hat{\mathbf{r}}$ explicitly in terms of the angles θ, ϕ:

$$Q\hat{\mathbf{r}} = \begin{bmatrix} Q_{xx} & Q_{xy} & Q_{xz} \\ Q_{yx} & Q_{yy} & Q_{yz} \\ Q_{zx} & Q_{zy} & Q_{zz} \end{bmatrix} \begin{bmatrix} \sin\theta\,\cos\phi \\ \sin\theta\,\sin\phi \\ \cos\theta \end{bmatrix}$$

17.12 Problems

17.1 *Computer Experiment—Dipoles.* Reproduce the results and graphs of Fig. 17.4.2, and calculate the corresponding directivities in dB.

17.2 Derive Eq. (17.3.7) for the input resistance of a dipole antenna.

17.3 Derive Eq. (17.6.6) for the tilt angle of a traveling wave antenna by reducing the problem to that of finding the maximum of the function $\sin^2(\pi x)/x$ in the interval $[0, 1]$.

17.4 *Computer Experiment–Traveling Wave Antennas.* Reproduce the results and graphs of Fig. 17.6.2.